Glycans on influenza hemagglutinin affect receptor binding and immune response

Cheng-Chi Wang[a,b,1], Juine-Ruey Chen[a,c,1], Yung-Chieh Tseng[a], Che-Hsiung Hsu[a,d,e], Yu-Fu Hung[a], Shih-Wei Chen[a], Chin-Mei Chen[f], Kay-Hooi Khoo[f], Ting-Jen Cheng[a], Yih-Shyun E. Cheng[a], Jia-Tsrong Jan[a], Chung-Yi Wu[a], Che Ma[a,2], and Chi-Huey Wong[a,2]

[a]Genomics Research Center, [d]Chemical Biology and Molecular Biophysics, Taiwan International Graduate Program, and [f]Institute of Biological Chemistry, Academia Sinica, Taipei 115, Taiwan; [b]Institute of Biochemical Sciences, National Taiwan University, Taipei 106, Taiwan; [c]Institute of Biochemistry and Molecular Biology, National Yang-Ming University, Taipei 112, Taiwan; and [e]Institute of Bioinformatics and Structural Biology, National Tsing Hua University, Hsinchu 300, Taiwan

Contributed by Chi-Huey Wong, September 1, 2009 (sent for review August 3, 2009)

Recent cases of avian influenza H5N1 and the swine-origin 2009 H1N1 have caused a great concern that a global disaster like the 1918 influenza pandemic may occur again. Viral transmission begins with a critical interaction between hemagglutinin (HA) glycoprotein, which is on the viral coat of influenza, and sialic acid (SA) containing glycans, which are on the host cell surface. To elucidate the role of HA glycosylation in this important interaction, various defined HA glycoforms were prepared, and their binding affinity and specificity were studied by using a synthetic SA microarray. Truncation of the N-glycan structures on HA increased SA binding affinities while decreasing specificity toward disparate SA ligands. The contribution of each monosaccharide and sulfate group within SA ligand structures to HA binding energy was quantitatively dissected. It was found that the sulfate group adds nearly 100-fold (2.04 kcal/mol) in binding energy to fully glycosylated HA, and so does the biantennary glycan to the monoglycosylated HA glycoform. Antibodies raised against HA protein bearing only a single N-linked GlcNAc at each glycosylation site showed better binding affinity and neutralization activity against influenza subtypes than the fully glycosylated HAs elicited. Thus, removal of structurally nonessential glycans on viral surface glycoproteins may be a very effective and general approach for vaccine design against influenza and other human viruses.

flu vaccine | glycan binding | glycosylation

The highly pathogenic H5N1 and the 2009 swine-origin influenza A (H1N1) viruses have caused global outbreaks and raised a great concern that further changes in the viruses may occur to bring about a deadly pandemic (1, 2). Important contributions to our understanding of influenza infections have come from the studies on hemagglutinin (HA), a viral coat glycoprotein that binds to specific sialylated glycan receptors in the respiratory tract, allowing the virus to enter the cell (3–6). To cross the species barrier and infect the human population, avian HA must change its receptor-binding preference from a terminally sialylated glycan that contains α2,3 (avian)-linked to α2,6 (human)-linked sialic acid motifs (7), and this switch could occur through only two mutations, as in the 1918 pandemic (8). Understanding the factors that affect influenza binding to glycan receptors is thus critical for developing methods to control any future crossover influenza strains that have pandemic potential.

HA is a homotrimeric transmembrane protein with an ectodomain composed of a globular head and a stem region (3). Both regions carry N-linked oligosaccharides (9), which affect the functional properties of HA (10, 11). Among different subtypes of influenza A viruses, there is extensive variation in the glycosylation sites of the head region, whereas the stem oligosaccharides are more conserved and required for fusion activity (11). Glycans near antigenic peptide epitopes interfere with antibody recognition (12), and glycans near the proteolytic activation site of HA modulate cleavage and influence the infectivity of influenza virus (13). Mutational deletion of HA glycosylation sites can affect viral receptor binding (14). Our analysis of HA sequences revealed that the peptide sequences around the glycosylation sites are highly conserved (Fig. S1), which suggests a central functional significance for HA glycosylation; however, little is known regarding how the structure and composition of its glycans affect HA activity, including structure, receptor binding, and immune response.

Results

Creating Defined HA Glycoforms for Quantitative Glycan Microarray Profiling. The glycan microarray is a powerful tool for investigating carbohydrate–protein interactions (15–18) and provides a new platform for influenza virus subtyping (16–18). Although powerful, understanding HA–glycan interactions by array analysis has been complicated by two issues. First, HA binding specificity is affected by the spatial arrangement and composition of the arrayed glycans and the binding detection method used (19). Second, the changes in the peptide sequence at or near glycosylation sites may alter HA's 3D structure, and thus receptor-binding specificity and affinity. Indeed, HAs from different H5N1 subtypes have different glycan-binding patterns (18). Mutagenesis of glycosylation sites on H1 and H3 has been studied in the whole-viral system (16, 20). However, it is not known how changes in glycosylation affect receptor-binding specificity and affinity, especially with regard to the most pathogenic H5N1 HA. To address this question, we have developed a glycan microarray comprising extensive structural analogs of the HA-binding ligand, and several defined glycoforms of HA were prepared by using the H5 consensus sequence (21) for quantitative binding analysis. Although previous studies have used HA from insect cell expression (16), glycosylation in insect cells differs from mammalian cells, with a marked difference being that complex type N-glycans terminating in galactose and sialic acid are not produced in insect cells. To generate native fully glycosylated HA variants (HA_{fg}), human embryonic kidney (HEK293) cells were used. To generate high-mannose-type glycosylation (HA_{hm}), HEK293S cells, which are deficient in *N*-acetylglucosaminyltransferase I ($GnTI^-$), were used. To further address the effect of HA glycan structure on HA receptor-binding affinity and specificity, sugar residues were enzymatically removed from the expressed HAs. Sialic acid residues were removed from HA_{fg} by neuraminidase (NA) treatment to pro-

Author contributions: C.-Y.W., C.M., and C.-H.W. designed research; C.-C.W., J.-R.C., Y.-C.T., C.-H.H., Y.-F.H., S.-W.C., C.-M.C., K.-H.K., and J.-T.J. performed research; T.-J.C. and Y.-S.E.C. contributed new reagents/analytic tools; C.-C.W. and J.-R.C. analyzed data; and C.-C.W., J.-R.C., C.-Y.W., C.M., and C.-H.W. wrote the paper.

The authors declare no conflict of interest.

[1]C.-C.W. and J.-R.C. contributed equally to this work.

[2]To whom correspondence may be addressed. E-mail: cma@gate.sinica.edu.tw or chwong@gate.sinica.edu.tw.

This article contains supporting information online at www.pnas.org/cgi/content/full/0909696106/DCSupplemental.

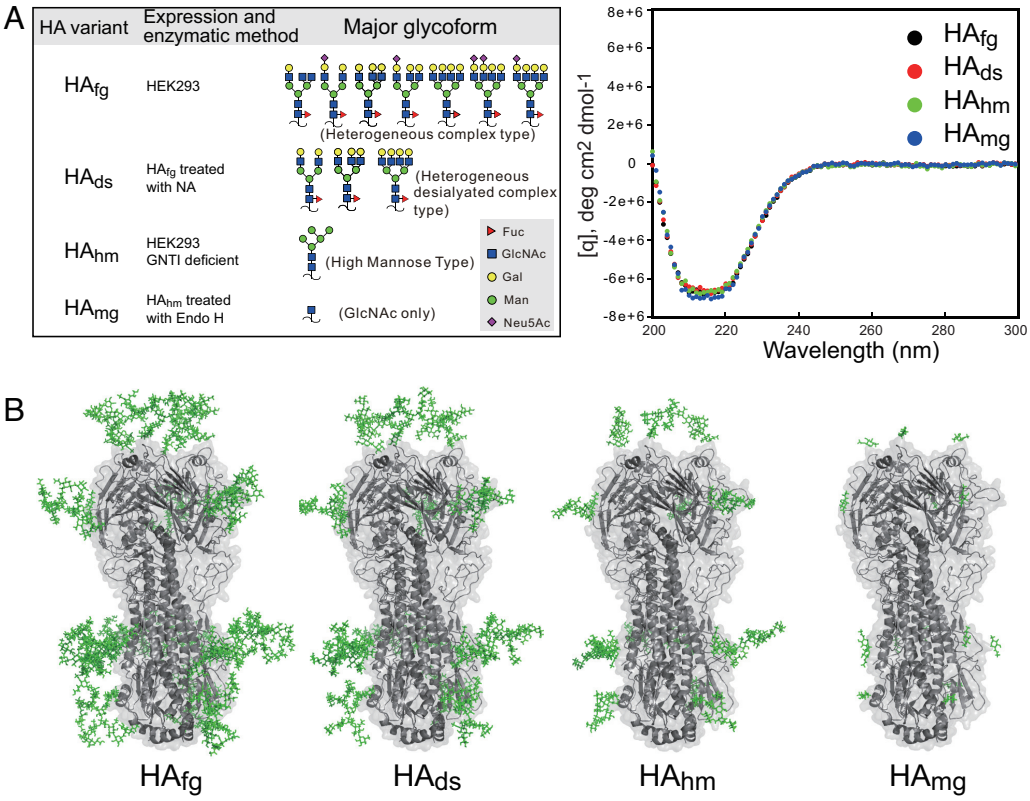

Fig. 1. Schematic overviews and circular dichroism spectra of HAs with different glycosylations. (*A*) Four variants of HA proteins with different glycosylations: HA_{fg}, HA [a consensus sequence (ref. 21) expressed in HEK293E cells with the typical complex type N-glycans]; HA_{ds}, NA-treated HA resulting in removal of sialic acids from HA_{fg}; HA_{hm}, HA expressed in GnTI$^-$ HEK293S cells with the high-mannose-type N-glycans; and HA_{mg}, Endo H-treated HA with GlcNAc only at its N-glycosylation sites. Circular dichroism spectra of HA_{fg}, HA_{ds}, HA_{hm}, and HA_{mg} demonstrate that the secondary structures of the four HA proteins with different glycosylations are similar. (*B*) Structure representation of HA_{fg}, HA_{ds}, HA_{hm}, and HA_{mg} with different N-glycans attached at their N-glycosylation sites. The protein structures are created with Protein Data Bank ID code 2FK0 (Viet04 HA), colored in gray, and the N-linked glycans are displayed in green. All N-glycans are modeled by GlyProt (39), and the graphics are generated by PyMOL (www.pymol.org).

duce desialylated HA (HA_{ds}). Endoglycosidase H (Endo H) was used to truncate all of the glycan structures down to a single GlcNAc residue to produce monoglycosylated HA (HA_{mg}). Thus, a total of four glycoform variants of HA were generated (Fig. 1 and Fig. S2), and the glycan structures are verified by mass spectral analysis (Figs. S3 and S4 and Table S1). Circular dichroism of the variants confirmed that their secondary structures are similar (Fig. 1*A*). It is noted that an attempt to express functional HA in *Escherichia coli* failed because of the lack of glycosylation.

The synthetic sialic acid glycan array consisted of 17 of the α2,3 (glycans **1–17**) and 7 of the α2,6 (glycans **21–27**) sialosides designed to explore the glycan specificity of influenza viruses (see Fig. 3). The synthetic sialosides with a five-carbon linker terminated with amine were prepared and covalently attached onto NHS-coated glass slides by forming an amide bond under aqueous conditions at room temperature. The printing procedure was based on the standard microarray robotic printing technology, as reported previously (15, 22). We applied the HA variants to the sialic acid slides and then hybridized them with primary antibody, followed by detection with a secondary antibody conjugated to Cy3. This analysis indicated that the H5N1 HA consensus sequence specifically binds to α2,3 sialosides but not α2,6 sialosides (Fig. 2*A*), in accordance with previous studies (16, 18). To our surprise, the binding strength with α2,3 sialosides grew successively stronger from HA_{fg}, HA_{ds}, and HA_{hm}, to HA_{mg} (Fig. 2*A*) by qualitative binding via relative fluorescence intensity.

We next prepared a quantitative array to determine surface dissociation constants (17). To avoid any skewing by antibody layering, HA was directly labeled with the fluorescent dye Cy3 (19). Direct binding assays were performed by serial dilution of Cy3-labeled HAs to establish the relative binding intensities. The dissociation constants on the surface were determined by plotting the HA concentrations against fluorescence intensity for each of the 24 sialosides printed on the glass slide. The dissociation constant $K_{D,surf}$ values were calculated based on the Langmuir isotherms (see Fig. 2*B* and Fig. S5). The monovalent HA–sialoside binding is weak, exhibiting dissociation constants in the millimolar range ($K_D = 2.5 \times 10^{-3}$ M) (23); however, HA is involved in multivalent interactions with sialosides on the host cell surface, which can be seen in the quantitative array profiling (Table 1).

All HA glycoforms showed strong binding to receptor glycans with a sulfate group at the 6 position of the third GlcNAc residue from the nonreducing end (glycans **4** and **7**). This sulfate group is important for binding to H5 HA (16, 18). In addition, it was observed that glycan **4** is the best ligand for HA_{fg}, whereas glycans **13–15** are better ligands than glycan **6** for HA_{mg}, indicating a possible multivalent interaction within the ligand-binding site, or the exposure of more receptor-binding domains to bigger biantennary sialosides (glycans **13** and **14**). Interestingly, HA binding substantially increases as its N-glycan structures become less complex (Fig. 2*B*). However, although the $K_{D,surf}$ values for HA_{mg} show stronger and similar binding to a few SA glycans, the other HA variants exhibit weaker and more specific binding to glycan ligands (Fig. 2*B* and Table S2). Thus, binding specificity and binding affinity may have an inverse relationship that is modulated by glycan structure. This modulation may have important biological signifi-

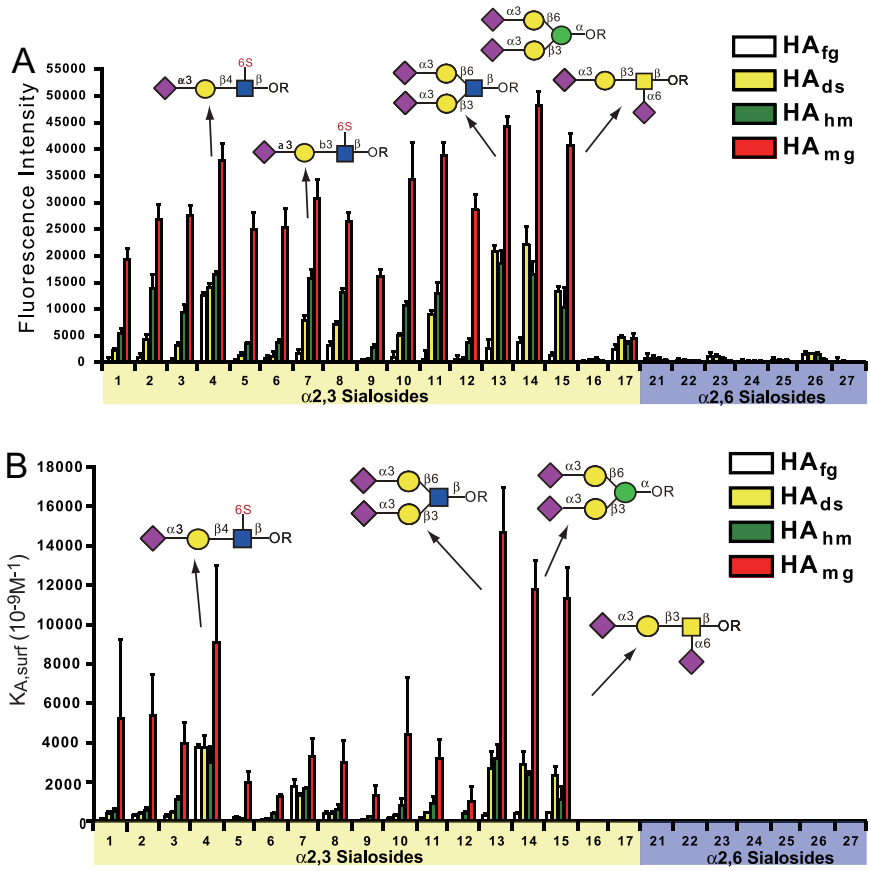

Fig. 2. Glycan microarray analysis of HA with different glycosylations. (*A*) Glycan microarray profiling of HA variants HA_{fg}, HA_{ds}, HA_{hm}, and HA_{mg} are shown. The related linkages of glycans were grouped by color, predominantly 17 α2,3 sialosides (yellow) or 7 α2,6 sialosides (blue). The structures of glycans on the array are indicated in Fig. 3. (*B*) Association constants of HA variants HA_{fg}, HA_{ds}, HA_{hm}, and HA_{mg} are shown with values of $K_{A,surf}$ of HA variants in response to α2,3 sialosides 1–15.

cance, in that the carbohydrates on HA can tune its recognition of glycan receptors on the lung epithelial cells.

Dissecting Binding Energy Contribution from Receptor Sialosides. The dissociation constant ($K_{D,surf}$) of HA–glycan interactions can be used to calculate the Gibbs free energy change of binding (ΔG_{multi}). Values for ΔG_{multi} represent a quantitative measurement of stabilizing energy from HA–glycan interactions. A successive decrease in ΔG_{multi} correlated with the systematic decrease in complexity/truncation of the N-glycan structures on HA (Table 1). The differences in free energy change ($\Delta\Delta G$) between HA variants are caused by unique glycan structures (Table S2), and the largest

Table 1. Dissociation constants ($K_{D,surf}$) and free energy changes (ΔG) of HA glycosylated variants when binding to α2,3 sialosides 1–15

	$K_{D,surf}$, μM ±SD					ΔG, kcal/mol ±SD				
Sialosides	HA_{fg}	HA_{fg}	HA_{fg}	HA_{fg}	ANOVA *P**	HA_{fg}	HA_{fg}	HA_{fg}	HA_{fg}
1	6.99 ± 0.41	2.86 ± 0.93	2.09 ± 0.59	0.27 ± 0.16	<0.0001	−7.03 ± 0.03	−7.58 ± 0.19	−7.76 ± 0.17	−8.80 ± 0.15
2	3.72 ± 1.01	2.47 ± 0.21	1.75 ± 0.32	0.20 ± 0.07	0.0002	−7.41 ± 0.16	−7.66 ± 0.06	−7.86 ± 0.11	−9.03 ± 0.07
3	4.55 ± 1.85	2.34 ± 0.27	0.92 ± 0.16	0.26 ± 0.06	0.0002	−7.31 ± 0.25	−7.68 ± 0.07	−8.24 ± 0.10	−8.90 ± 0.01
4	0.27 ± 0.01	0.27 ± 0.05	0.33 ± 0.09	0.13 ± 0.06	0.0048	−8.96 ± 0.03	−8.95 ± 0.10	−8.84 ± 0.16	−9.45 ± 0.27
5	ND	5.20 ± 1.01	9.40 ± 3.20	0.54 ± 0.15	ND	ND	−7.21 ± 0.11	−6.88 ± 0.21	−8.49 ± 0.13
6	20.03 ± 4.24	9.22 ± 2.05	2.71 ± 0.53	0.80 ± 0.05	<0.0001	−6.41 ± 0.13	−6.87 ± 0.13	−7.65 ± 0.06	−8.32 ± 0.05
7	0.57 ± 0.10	0.77 ± 0.08	0.61 ± 0.02	0.32 ± 0.10	0.0010	−8.46 ± 0.06	−8.36 ± 0.04	−8.47 ± 0.02	−8.78 ± 0.14
8	2.49 ± 0.58	2.48 ± 0.41	1.69 ± 0.53	0.36 ± 0.13	0.0008	−7.65 ± 0.14	−7.65 ± 0.10	−7.89 ± 0.21	−8.82 ± 0.30
9	ND	15.34 ± 5.06	4.40 ± 0.56	0.86 ± 0.34	ND	ND	−6.58 ± 0.20	−7.31 ± 0.08	−8.18 ± 0.16
10	7.64 ± 2.3	3.61 ± 0.61	1.22 ± 0.52	0.29 ± 0.14	0.0003	−6.99 ± 0.18	−7.43 ± 0.10	−8.09 ± 0.24	−8.77 ± 0.03
11	6.02 ± 1.04	2.32 ± 0.14	1.11 ± 0.51	0.33 ± 0.08	<0.0001	−7.12 ± 0.10	−7.68 ± 0.04	−8.15 ± 0.25	−8.91 ± 0.18
12	40.23 ± 9.77	ND	2.45 ± 0.52	1.41 ± 0.92	ND	−6.00 ± 0.15	ND	−7.66 ± 0.12	−7.85 ± 0.25
13	3.38 ± 1.06	1.37 ± 0.30	0.31 ± 0.06	0.07 ± 0.01	0.0008	−7.47 ± 0.19	−8.05 ± 0.13	−8.88 ± 0.13	−9.77 ± 0.09
14	2.72 ± 0.41	0.97 ± 0.41	0.42 ± 0.03	0.09 ± 0.01	<0.0001	−7.59 ± 0.09	−8.27 ± 0.28	−8.69 ± 0.04	−9.60 ± 0.01
15	2.37 ± 0.19	1.32 ± 0.16	0.89 ± 0.35	0.09 ± 0.01	0.0002	−7.67 ± 0.05	−8.02 ± 0.07	−8.29 ± 0.27	−9.62 ± 0.08

Thermodynamic parameters of HA with different glycosylations in response to α2,3 sialosides 1–15. Free energy changes (ΔG) and $K_{D,surf}$ of HA–glycan interactions are shown in response to α2,3 sialosides 1–15. ΔG values can be derived from $K_{D,surf}$ values by using the equation $\Delta G_{multi} = -RT\ ln\ (K_{D,surf}^{-1})$. The values of ΔG were calculated according to $K_{D,surf}$ values to obtain free energy changes in HA–glycan binding. $\Delta G(HA_{fg})$ of glycans **5** and **9** is not determined. ND indicates not determined.

*From the set of 15 identified HA-binding sialosides, statistically significant differences of $K_{D,surf}$ values among four HA glycoforms are shown by using a one-way ANOVA ($P < 0.05$ is significant).

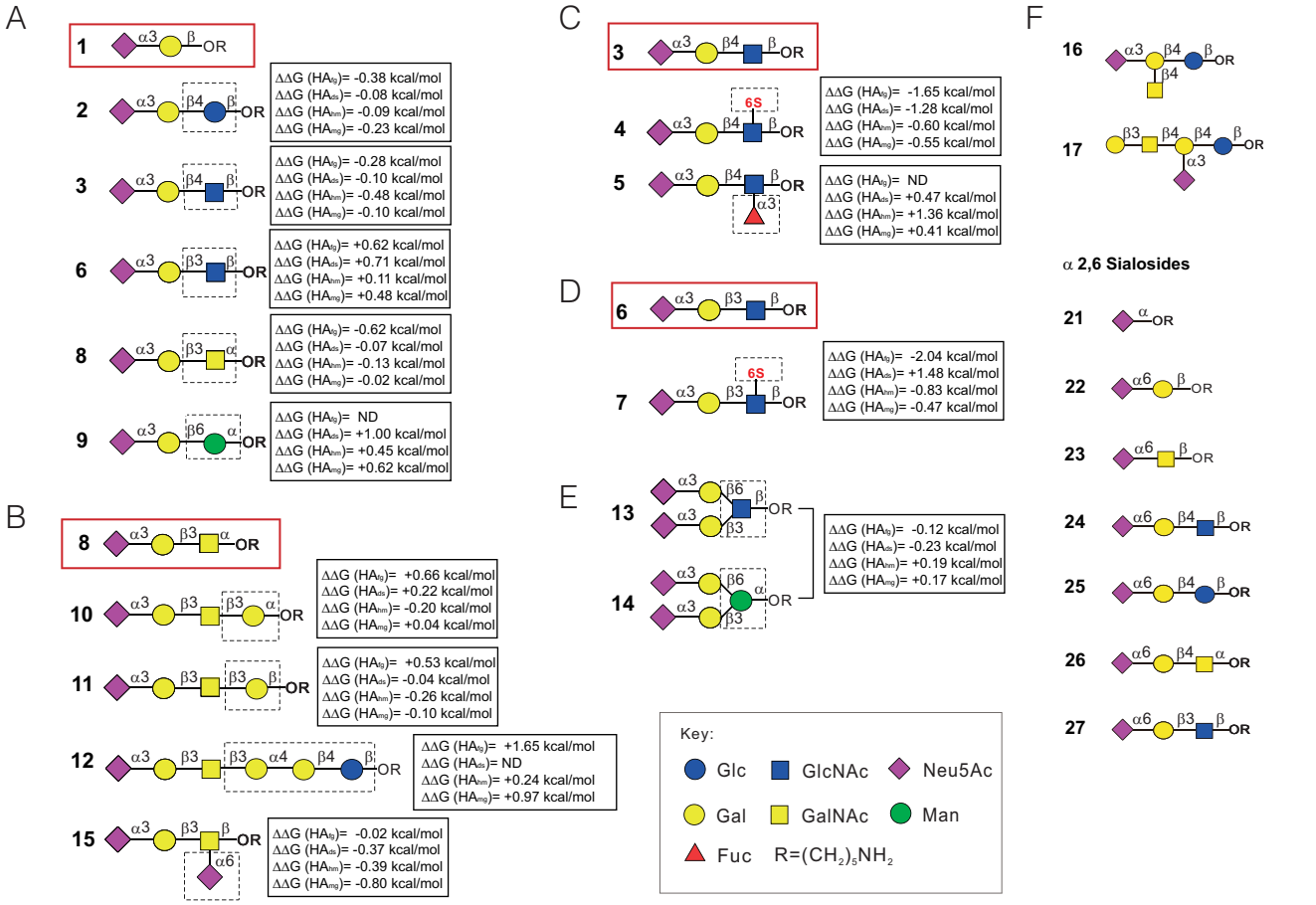

Fig. 3. The binding energy contributions from sugars or modifications of HA–glycan interactions in response to HAs with different glycosylations. These values were obtained by subtraction of ΔG values of the indicated reference glycan (highlighted in red boxes; see Table S3). (*A*) Glycans **2**, **3**, **6**, and **8**–**10** possess the same backbone of the disaccharide glycan **1** but only differ in the third sugar from the nonreducing end. The values of ΔΔG are calculated to demonstrate the binding energy difference by changing the third sugars. (*B*) Glycans **10**–**12** and **15** possess the same backbone of the disaccharide glycan **8** but differ either by elongating the sugar structure linearly or by adding a branched sugar. (*C*) Glycans **4** and **5** possess the same backbone of the trisaccharide glycan **3** but differ either by the branched fucose or the sulfate group on the third position from the nonreducing end. (*D*) Glycans **6** and **7** differ in the sulfate group on the third position from the nonreducing end of glycan **7**. (*E*) Glycans **13** and **14** are α2,3 biantennary sialosides but differ in the change of the internal sugar. (*F*) Glycans **16** and **17** and α2,6 sialosides (nos. 21–27) show little or no binding to HA.

difference is between HA_{fg} and HA_{mg} ($\Delta\Delta G$ $HA_{fg} \rightarrow HA_{mg}$; see Table S2), which is consistent with the largest difference in binding energy resulting from trimming off most of the N-glycan down to a single GlcNAc. It is noted that values of ΔΔG are similar except for glycans **4** and **7** (Table S2), indicating that glycans on HA do not significantly affect the binding affinity with sulfated α2,3 trisaccharide (16).

The molecular details of the HA–receptor binding (i.e., the contribution from each structural component comprising a glycan receptor) can be addressed by comparing the differences in free energy change (ΔΔG values) between different receptor sialosides (Fig. 3 and Table S3). Dissecting the energy contribution of the receptor sialosides responsible for HA binding will reveal key points of specificity that can be used to design new HA inhibitors. Sialosides α2,3 linked to galactose residues with β1,4 (Galβ1–4) linkages possess better binding affinity than those with Galβ1–3 linkages (18). This is reflected in the comparison of the Neu5Acα2,3-galactose (Neu5Acα2,3Gal) disaccharide backbone (Fig. 3*A*, glycan **1**, red box highlight), where trisaccharides **3** and **6** only differ in the linkage between Gal and GlcNAc. Here, the ΔΔG(**1** → **3**) for all HA variants is negative (stabilizing HA–receptor interaction), whereas the ΔΔG(**1** → **6**) for all HA variants is positive (destabilizing HA–receptor interaction; Fig. 3*A* and Table S3). This observation indicates that Neu5Acα2,3Galβ1–4Glc/GlcNAc is the core glycan component interacting with the HA-binding pocket. Moreover, the value of ΔΔG(**1** → **9**) for all HA variants is positive, indicating a negative perturbation caused by the β6-linked mannose at the third position (Fig. 3*A* and Table S3). Thus, binding energy is affected by inner sugar residues and their linkage patterns to the distal Neu5Acα2,3Gal disaccharide ligand (Fig. 3*A*). This analysis shows that a GlcNAc residue at the third position is favored for all HA variants. However, in comparing ΔΔG values for glycans **13** and **14** (Fig. 3*E* and Table S3) to glycan **6**, multivalent interactions in the binding site with the biantennary sialoside are apparent, and for HA_{mg}, this intramolecular avidity is more significant for driving binding than the structural effect exerted by the third sugar.

Next, we compared receptor glycans **10**, **11**, **12**, and **15**, which have the same basic core structure (glycan **8** trisaccharide) but differ by elongation (glycans **11** and **12**) or addition of an α2,6 sialic acid at the third position (glycan **15**; Fig. 3*B*). It is interesting that the sialoside with the branched α2,6 sialic acid greatly increased HA avidity, whereas the longer α2,3 sialoside extending from glycan **8** resulted in a weaker binding by HAs [ΔΔG (**8** → **15**) > ΔΔG (**8** → **11**) ~ ΔΔG (**8** → **10**) > ΔΔG (**8** → **12**); Fig. 3*B* and Table S3].

Glycans **3**–**5** snd **6**–**7** share the same trisaccharide backbone but differ by the addition of a sulfate group (glycan **4**) or fucose residue (glycan **5**) on the third GlcNAc from the nonreducing end. The sulfate group can stabilize the HA–receptor glycan interaction up

to 2.044 kcal/mol [ΔΔG (**6** → **7**)], the largest energy gap between two receptor sialosides. Among all of the HA variants, the fully glycosylated variant showed the most significant differences in free energy changes, with values of ΔΔG(**3** → **4**) HA_{fg} (−1.653 kcal/mol) and ΔΔG(**6** → **7**) HA_{fg} (−2.044 kcal/mol), and the size of the free energy gain lessened as the glycan structure became more simplified; i.e., $HA_{fg} > HA_{ds} > HA_{hm} > HA_{mg}$. Thus, sulfated glycans dramatically enhance HA binding, and fully glycosylated HA maximizes this effect (Fig. 3 *C* and *D*), which may be important for H5N1 pathogenesis. On the other hand, the fucosylated receptor analogs greatly destabilize HA binding, with all glycosylated HA variants showing a positive ΔΔG(**3** → **5**) (Fig. 3*C*). These large differences in ΔΔG(**3** → **4**) and ΔΔG(**3** → **5**) are likely caused by an important binding interaction in the receptor-binding pocket, which the sulfate group maximizes and the fucose sterically blocks. The weak binding of HA_{fg} is unlikely due to the competition of its sialylglycans, because removal of sialic acid has a small effect on binding, and HA_{fg} still exhibits a strong affinity for certain specific sialylglycans.

Vaccine Design Using Monoglycosylated HA. The monoglycosylated hemagglutinin HA_{mg} described in this work shows a similar secondary structure and better binding affinity to host receptors compared with its fully glycosylated counterpart. Our recent study also indicated that a single GlcNAc residue to Asn is the minimum component of the N-glycan required for glycoprotein folding and stabilization (24). Because proteins are superior immunogens to glycans, the monoglycosylated HA was tested as a protein vaccine against influenza viruses. Antisera from HA_{fg} and HA_{mg} immunizations were compared with regard to their ability to bind native HAs and to neutralize H5 viruses (Fig. 4). Indeed, in contrast to HA_{fg}, the antiserum from HA_{mg} showed stronger neutralization of the virus. The HA_{mg} antiserum also binds to H1 (New Caledonia/1999) in addition to the H5 subtypes Vietnam/1194, H5 (Anhui), and H5 (ID5/2005) (Fig. S6). Notably, the HA_{mg} vaccine was much more protective than the HA_{fg} vaccine in a challenge study (Fig. 4*C*). The amino acid sequences of H1, H3, and H5 isolated from humans since 1918 were compared (Fig. S1). The overall sequence identity was about 65% between H1 and H5, and about 40% between H3 and H5. In addition, the glycosylation sites and the underlying peptide sequences between H1 and H5 were more conserved compared with those between H3 and H5.

Discussion

This study shows that the systematic simplification of N-glycans on HA results in a successive increase in binding to α2,3 sialosides but not to α2,6 sialosides. To our knowledge, this is a previously undescribed study to show the effect of HA's outer and inner glycans on receptor binding and to quantitatively dissect the binding affinity and energetic contributions of HA–receptor interactions.

HA glycosylation affects the function of influenza HA (25). Interestingly, as the level of glycosylation on influenza H3N2 has increased since 1968, the morbidity, mortality, and viral lung titers have decreased (26). Our finding that HA with a single GlcNAc attached to the glycosylation sites showed relaxed specificity but enhanced affinity to α2,3 sialosides suggests that the N-glycans on HA may cause steric hindrance near the HA–receptor binding domain. The high specificity for receptor sialosides may prevent the virus from binding to some other specific glycans on the human lung epithelial cell surface. On the other hand, HA with truncated glycans can recognize α2,3 receptor sialosides with higher binding affinity and less specificity, suggesting that reducing the length of glycans on HA may increase the risk of avian flu infection. It is, however, unclear how the changes of HA–receptor interaction via glycosylation affect the infectivity of the virus and the NA activity in the viral life cycle.

HA with a single GlcNAc is a promising candidate for influenza vaccine because such a construct retains the intact structure of HA and can be easily prepared (e.g., via yeast). It also can expose conserved epitopes hidden by large glycans to elicit an immune response that recognizes HA variants in higher titer. This strategy opens a new direction for vaccine design and, together with other different vaccine strategies (27–30) and recent discoveries of HA-neutralizing antibodies (31–36), should facilitate the development of vaccines against viruses such as influenza, hepatitis C virus, and HIV.

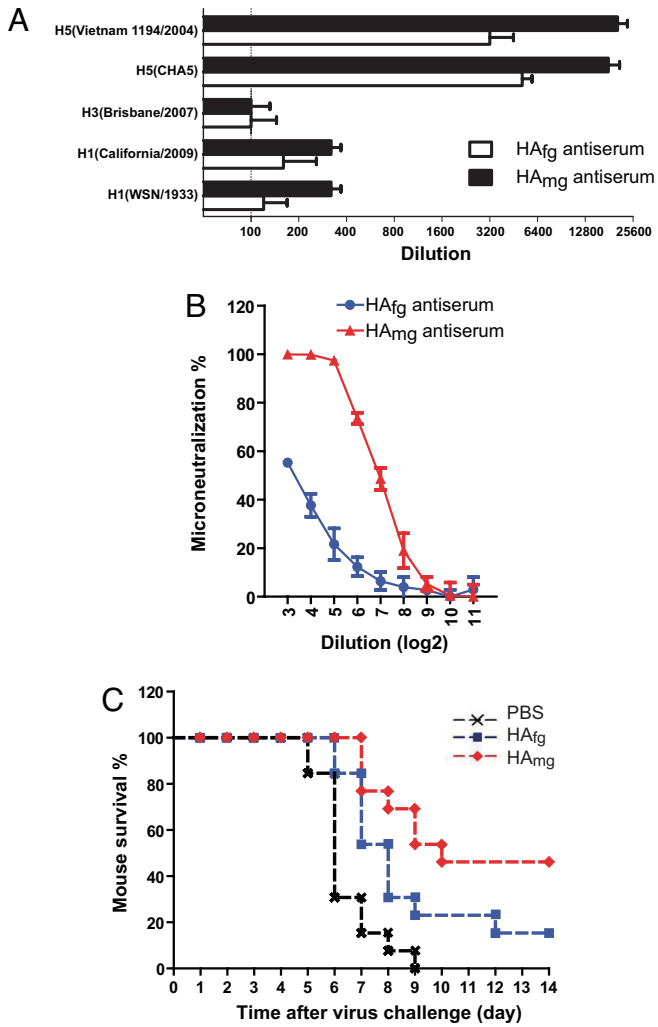

Fig. 4. Comparison of HA_{fg} and HA_{mg} as vaccine. (*A*) The bindings between antisera from HA_{fg} and HA_{mg}, and various HAs are analyzed by using ELISA. In comparison with HA_{fg} antiserum, HA_{mg} antiserum shows better binding to H5 (Vietnam 1194/2004 and CHA5). In addition, the HA_{mg} antiserum also binds to H1 (California 07/2009 and WSN). (*B*) Microneutralization of H5N1 (NIBRG-14) virus with HA_{fg} and HA_{mg} antisera. In comparison with HA_{fg} antiserum, HA_{mg} antiserum shows better neutralizing activity against influenza virus infection to MDCK cells ($P < 0.0001$). (*C*) Vaccine protection against lethal-dose challenge of H5N1 virus. BALB/c mice were immunized with two injections of the HA protein vaccine HA_{fg}, HA_{mg}, and control PBS. The immunized mice were intranasally challenged with a lethal dose of H5N1 (NIBRG-14) virus. After challenge, the survival was recorded for 14 days.

Materials and Methods

Protein Expression and Purification. The plasmid that encodes the secreted HA was transfected into the human embryonic kidney cell lines of either HEK293EBNA (ATCC number CRL-10852) or the GnTI$^-$ HEK293S cells (37) by using polyethyleneimine and was cultured in Freestyle 293 expression medium (Invitrogen) supplemented with 0.5% bovine calf serum. The supernatant was collected 72 h after transfection and cleared by centrifugation. HA proteins were purified with

Nickel-chelation chromatography as previously described (38) to obtain fully glycosylated HA_{fg} and high-mannose-type HA_{hm}. To obtain the HA protein without sialylation—the desialylated HA_{ds}—the purified protein was treated with 20 mM *Clostridium* NA (Sigma) for 2 h at 37 °C. After the NA treatment, the protein was purified again to be separated from the NA. The purified HA_{hm} was treated with Endo H (NEB) for 2 h at 37 °C to produce HA protein with a single GlcNAc at the glycosylation sites, the monoglycosylated HA_{mg}.

Glycan Microarray Fabrication. Twenty-four sialic acid-containing glycans designed for HAs were prepared chemically and used for array fabrication. Microarrays were printed (BioDot; Cartesian Technologies) by robotic pin (SMP3; TeleChem International) deposition of ≈0.7 nL of various concentrations of amine-containing glycans in printing buffer (300 mM phosphate buffer, pH 8.5, containing 0.005% Tween 20) from a 384-well plate onto NHS-coated glass slides (Nexterion H slide; SCHOTT North America). The slides for sialosides were spotted with solutions of glycans **1–17** and **21–27** with concentrations of 100 μM in each row for one glycan from bottom to top, with 12 replicates horizontally placed in each subarray, and each slide was designed for 16 grids for further incubation experiments. Printed slides were allowed to react in an atmosphere of 80% humidity for an hour followed by desiccation overnight, and they were stored at room temperature in a desiccator until use. Before the binding assay, these slides were blocked with ethanolamine (50 mM ethanolamine in borate buffer, pH 9.2) and then washed with water and PBS buffer, pH 7.4, twice.

Indirect Binding Assay. HA glycosylated variants were prepared in 0.005% Tween 20/PBS buffer, pH 7.4, and added to cover the grid on glycan array with application of a coverslip. After incubation in a humidified chamber with shaking for 1 h, the slides were washed three times with 0.005% Tween 20/PBS buffer, pH 7.4. Next, rabbit anti-H5N1 HA antibody was added to the slides and incubated in a humidified chamber for 1 h. After washing the slides with 0.005% Tween 20/PBS buffer three times, Cy3-conjugated goat anti-rabbit IgG antibody was added to the slides and incubated in a humidified chamber for another 1 h. The slides were washed three times with 0.05% Tween 20/PBS buffer, pH 7.4; three times with PBS buffer, pH 7.4; and three times with H_2O, and then dried. The slides were scanned at 595 nm (for Cy3) with a microarray fluorescence chip reader (GenePix Pro 6.0; Molecular Devices).

Direct Binding Assay. Cy3-labeled HA proteins with different glycosylations were prepared in 0.005% Tween 20/PBS buffer, pH 7.4, and added to cover the grid on glycan array with application of a coverslip. After incubation in a humidified chamber with shaking for 1 h, the slides were washed three times with 0.005% Tween 20/PBS buffer, pH 7.4; three times with PBS buffer, pH 7.4; and three times with H_2O, and then dried. The slides were scanned at 595 nm (for Cy3) with a microarray fluorescence chip reader (GenePix Pro 6.0; Molecular Devices).

Microneutralization Assay. The freshly prepared H5N1 (NIBRG-14) virus (National Institute for Biological Standards and Control, Potters Bar, U.K.) was quantified with the median tissue culture infectious dose ($TCID_{50}$). The 100-fold $TCID_{50}$ of virus was mixed in equal volume with 2-fold serial dilutions of serum stock solution in 96-well plates and incubated for 1 h at 37 °C. The mixture was added onto the MDCK cells (1.5×10^4 cells per well) on the plates, followed by incubation at 37 °C for 16–20 h. The cells were washed with PBS, fixed in acetone/methanol solution (vol/vol 1:1), and blocked with 5% skim milk. The viral antigen was detected by indirect ELISA with an mAb against influenza A NP (35).

Mice, Vaccination, and Challenge. Female 6- to 8-week-old BALB/c mice (n = 15) were immunized intramuscularly with 20 μg of purified HA_{fg} or HA_{mg} proteins in 50 μL of PBS, pH 7.4, and mixed with 50 μL of 1 mg/mL aluminum hydroxide (Alum; Sigma) at weeks 0 and 2. Blood was collected 14 days after immunization, and serum samples were collected from each mouse. The immunized mice were challenged intranasally with a genetically modified H5N1 virus, NIBRG-14, with a lethal dose (100-fold lethal dose to 50% of mice). The mice were monitored daily for 14 days after the challenge for survival. All animal experiments were evaluated and approved by the Institutional Animal Care and Use Committee of Academia Sinica.

ACKNOWLEDGMENTS. We sincerely thank S.-H. Ma for virus challenge experiments, C.-Y. Su and S.-Y. Wang for virus neutralization experiments, and P. J. Reeves (University of Essex, United Kingdom) for providing $GnTI^-$ HEK293S cells. We thank Academia Sinica for financial support. MALDI-MS profiles of the N-glycans were acquired at the National Research Program for Genomic Medicine Core Facilities for Proteomics and Glycomics, supported by the Taiwan National Science Council.

1. Garten RJ, et al. (2009) Antigenic and genetic characteristics of swine-origin 2009 A(H1N1) influenza viruses circulating in humans. *Science* 325:197–201.
2. Neumann G, Noda T, Kawaoka Y (2009) Emergence and pandemic potential of swine-origin H1N1 influenza virus. *Nature* 459:931–939.
3. Kuiken T, et al. (2006) Host species barriers to influenza virus infections. *Science* 312:394–397.
4. Maines TR, et al. (2009) Transmission and pathogenesis of swine-origin 2009 A(H1N1) influenza viruses in ferrets and mice. *Science* 325:484–487.
5. Skehel JJ, Wiley DC (2000) Receptor binding and membrane fusion in virus entry: The influenza hemagglutinin. *Annu Rev Biochem* 69:531–569.
6. van Riel D, et al. (2006) H5N1 virus attachment to lower respiratory tract. *Science* 312:399–399.
7. Connor RJ, Kawaoka Y, Webster RG, Paulson JC (1994) Receptor specificity in human, avian, and equine H2 and H3 influenza virus isolates. *Virology* 205:17–23.
8. Tumpey TM, et al. (2007) A two-amino acid change in the hemagglutinin of the 1918 influenza virus abolishes transmission. *Science* 315:655–659.
9. Keil W, et al. (1985) Carbohydrates of influenza-virus–structural elucidation of the individual glycans of the FPV hemagglutinin by two-dimensional H-1 NMR and methylation analysis. *EMBO J* 4:2711–2720.
10. Chen ZY, Aspelund A, Jin H (2008) Stabilizing the glycosylation pattern of influenza B hemagglutinin following adaptation to growth in eggs. *Vaccine* 26:361–371.
11. Ohuchi R, Ohuchi M, Garten W, Klenk HD (1997) Oligosaccharides in the stem region maintain the influenza virus hemagglutinin in the metastable form required for fusion activity. *J Virol* 71:3719–3725.
12. Skehel JJ, et al. (1984) A carbohydrate side-chain on hemagglutinins of Hong Kong influenza-viruses inhibits recognition by a monoclonal-antiboby. *Proc Natl Acad Sci USA* 81:1779–1783.
13. Deshpande KL, Fried VA, Ando M, Webster RG (1987) Glycosylation affects cleavage of an H5N2 influenza-virus hemagglutinin and regulates virulence. *Proc Natl Acad Sci USA* 84:36–40.
14. Gunther I, Glatthaar B, Doller G, Garten W (1993) A H1-hemagglutinin of a human influenza A-virus with a carbohydrate-modulated receptor-binding site and an unusual cleavage site. *Virus Res* 27:147–160.
15. Blixt O, et al. (2004) Printed covalent glycan array for ligand profiling of diverse glycan binding proteins. *Proc Natl Acad Sci USA* 101:17033–17038.
16. Chandrasekaran A, et al. (2008) Glycan topology determines human adaptation of avian H5N1 virus hemagglutinin. *Nat Biotechnol* 26:107–113.
17. Liang PH, Wang SK, Wong CH (2007) Quantitative analysis of carbohydrate-protein interactions using glycan microarrays: Determination of surface and solution dissociation constants. *J Am Chem Soc* 129:11177–11184.
18. Stevens J, et al. (2008) Recent avian H5N1 viruses exhibit increased propensity for acquiring human receptor specificity. *J Mol Biol* 381:1382–1394.
19. Srinivasan A, et al. (2008) Quantitative biochemical rationale for differences in transmissibility of 1918 pandemic influenza A viruses. *Proc Natl Acad Sci USA* 105:2800–2805.
20. Deom CM, Caton AJ, Schulze IT (1986) Host cell-mediated selection of a mutant influenza A virus that has lost a complex oligosaccharide from the tip of the hemagglutinin. *Proc Natl Acad Sci USA* 83:3771–3775.
21. Chen MW, et al. (2008) A consensus-hemagglutinin-based DNA vaccine that protects mice against divergent H5N1 influenza viruses. *Proc Natl Acad Sci USA* 105:13538–13543.
22. Wang CC, et al. (2008) Glycan microarray of Globo H and related structures for quantitative analysis of breast cancer. *Proc Natl Acad Sci USA* 105:11661–11666.
23. Sauter NK, et al. (1989) Hemagglutinins from 2 influenza-virus variants bind to sialic-acid derivatives with millimolar dissociation-constants - A 500-MHz proton nuclear magnetic-resonance study. *Biochemistry* 28:8388–8396.
24. Hanson SR, et al. (2009) The core trisaccharide of an N-linked glycoprotein intrinsically accelerates folding and enhances stability. *Proc Natl Acad Sci USA* 106:3131–3136.
25. Wagner R, Heuer D, Wolff T, Herwig A, Klenk HD (2002) N-glycans attached to the stem domain of haemagglutinin efficiently regulate influenza A virus replication. *J Gen Virol* 83:601–609.
26. Vigerust DJ, et al. (2007) N-linked glycosylation attenuates H3N2 influenza viruses. *J Virol* 81:8593–8600.
27. Hoffmann E, Lipatov AS, Webby RJ, Govorkova EA, Webster RG (2005) Role of specific hemagglutinin amino acids in the immunogenicity and protection of H5N1 influenza virus vaccines. *Proc Natl Acad Sci USA* 102:12915–12920.
28. Huleatt JW, et al. (2008) Potent immunogenicity and efficacy of a universal influenza vaccine candidate comprising a recombinant fusion protein linking influenza M2e to the TLR5 ligand flagellin. *Vaccine* 26:201–214.
29. Scanlan CN, et al. (2007) Inhibition of mammalian glycan biosynthesis produces non-self antigens for a broadly neutralising, HIV-1 specific antibody. *J Mol Biol* 372:16–22.
30. Yang ZY, et al. (2007) Immunization by avian H5 influenza hemagglutinin mutants with altered receptor binding specificity. *Science* 317:825–828.
31. Ekiert DC, et al. (2009) Antibody recognition of a highly conserved influenza virus epitope. *Science* 324:246–251.
32. Kashyap AK, et al. (2008) Combinatorial antibody libraries from survivors of the Turkish H5N1 avian influenza outbreak reveal virus neutralization strategies. *Proc Natl Acad Sci USA* 105:5986–5991.
33. Scheid JF, et al. (2009) Broad diversity of neutralizing antibodies isolated from memory B cells in HIV-infected individuals. *Nature* 458:636–640.
34. Stevens J, et al. (2006) Structure and receptor specificity of the hemagglutinin from an H5N1 influenza virus. *Science* 312:404–410.
35. Sui JH, et al. (2009) Structural and functional bases for broad-spectrum neutralization of avian and human influenza A viruses. *Nat Struct Mol Biol* 16:265–273.
36. Throsby M, et al. (2008) Heterosubtypic neutralizing monoclonal antibodies cross-protective against H5N1 and H1N1 recovered from human IgM memory B cells. *PLoS ONE* 3:e3942.
37. Reeves PJ, Callewaert N, Contreras R, Khorana HG (2002) Structure and function in rhodopsin: High-level expression of rhodopsin with restricted and homogeneous N-glycosylation by a tetracycline-inducible N-acetylglucosaminyltransferase I-negative HEK293S stable mammalian cell line. *Proc Natl Acad Sci USA* 99:13419–13424.
38. Wei CJ, et al. (2008) Comparative efficacy of neutralizing antibodies elicited by recombinant hemagglutinin proteins from avian H5N1 influenza virus. *J Virol* 82:6200–6208.
39. Bohne-Lang A, von der Lieth CW (2005) GlyProt: In silico glycosylation of proteins. *Nucleic Acids Res* 33:W214–W219.